Building Simulation 2009

Eleventh International IBPSA Conference
Glasgow, Scotland
July 27-30, 2009

STUDY OF THE TRANSIENT BEHAVIOUR OF A HEMP CONCRETE BUILDING ENVELOPE

A.D. Tran Le[1] - C. Maalouf[1] - T.H. Mai[1] - E. Wurtz[2]

[1]LTM. - Laboratoire de Thermomécanique, GRESPI, Université de Reims
Faculté des Sciences, BP. 1039, Moulin de la Housse,
F-51687 Reims, Cedex 2, France.
[2]INES, Savoie Technolac, 50 Avenue du lac Leman, BP 332,
73375 Le Bourget du Lac, France.

ABSTRACT

Hemp concrete is more and more recommended by eco-builders because hemp is a renewable plant, recyclable and does not degrade within time. To integrate this material into buildings, it is important to study its hygrothermal behaviour. In this paper, two models have been investigated: a heat transfer model (**Th**) and a hygrothermal model accounting for heat and moisture transport through building envelope (**HAM**). Both models were implemented into the simulation environment SPARK. Simulations were run for a room located in Nancy and for winter conditions. Our results suggest that hemp concrete has a good thermal performance. Its low conductivity reduces energy consumption. Besides its moisture buffering capacity dampens indoor relative humidity variation.

INTRODUCTION

The sustainable world's economic growth and people' s life improvement greatly depend on the use of alternative products in the architecture and construction, such as vegetal fibers conventionally called green materials. Among these materials, hemp is the most used in the construction. Its application is still limited. The researches done until this day ((Collet, 2004), (Cerezo, 2005), (Elfordy, 200)) allowed us to determine its physical properties. In comparison with other materials in construction, the hemp concrete has a low heat conductivity (0,06-0,18 W/m.K), which reduces heat diffusion and thus reduces winter heat losses and protects from summer heat waves. Though it has a low mass density (200-800 kg/m^3), which reduces its storage capacity, its density remains higher than classical insulation materials. Besides, since hemp concrete is a hygroscopic material, it has the capacity to store or release moisture to ambiance air so it has ability to moderate the daily or seasonal humidity variations of the indoor environment and even the ability to moderate sudden step change of an indoor moisture level. Furthermore, the grey energy of hemp concrete is 90 kWh/m^3 and it is lower than normal concrete and brick grey energy which are respectively 430 kWh/m^3 and 696 kWh/m^3. Regarding all that, hemp concrete can be considered as a good compromise between insulation, energy efficiency, buffering capacity purpose and green material. However, these aspects reflect partially the comfort felt in buildings constructed with hemp concrete, its role of hygrothermal regulator is difficult to quantify and we rarely find, in the literature, studies concerning the use of these vegetable materials in construction.

The purpose of this paper is to study hemp concrete performance when used as building envelope. First, we present the mathematical models for building envelope and their implementation in SPARK, a program oriented object suited to complex problems (Sowell et al., 2001). Then we present simulation results. Two studies are shown: one takes into account only heat transfer through walls and compares the use of hemp concrete with normal concrete and another one takes into account heat and moisture transfer in hemp concrete.

MATHEMATICAL MODELS

In this section, we present the mathematical model for the heat and moisture transfer model (**HAM**). In order to model heat and mass transfer in buildings we used a nodal method, which considers that every zone of a building is perfectly mixed. Therefore, every zone can be characterized by a pressure, a temperature and a moisture concentration. A nodal method involves equations for air and moisture mass balance, heat balance for ambiance and equations describing heat and mass transfer through the walls, additional convection between inside wall surfaces and room ambiance and radiation exchange between inside wall surfaces. In the following sections, we detail these equations.

Moisture transport in building materials

Regarding indoor thermal comfort, relative humidity is an important parameter influencing perceived indoor air quality and human comfort. High moisture levels can damage construction and inhabitant's health. High humidity harms materials, especially in

case of condensation and it helps moulds development increasing allergic risks. Consequently, several researchers have studied the use of various hygroscopic materials to moderate indoor humidity levels. The material that absorbs and desorbs water vapour can be used to moderate the amplitude of indoor relative humidity and therefore to participate in the improvement of the indoor quality and energy saving. ((Olalekan et al., 2006), (Kwiatkowski et al., 2009), (Hameury, 2005)).

Mechanisms of moisture transport in a single building material have been extensively studied ((Künzel, 1995), (Perdesen, 1992), (Mendes et al., 1997)). Most of the models have nearly the same origin Philip and de Vries model (Philip and al., 1957). In this article, we use the Umidus model (Mendes et al., 1997) in which moisture is transported under liquid and vapour phases. Forms of moisture transport depend on the pore structure as well as environmental condition. The liquid phase is transported by capillarity whereas the vapour phase is due to the gradients of partial vapour pressure. With these considerations, the mass conservation equation becomes:

$$\frac{\partial \theta}{\partial \tau} = \frac{\partial}{\partial x}\left(D_T \frac{\partial T}{\partial x} \right) + \frac{\partial}{\partial x}\left(D_\theta \frac{\partial \theta}{\partial x} \right) \quad (1)$$

With the boundary conditions (x=0 and x=L):

$$-\rho_l \left(D_T \frac{\partial T}{\partial x} + D_\theta \frac{\partial \theta}{\partial x} \right)\Bigg|_{x=0,e} = h_{M,e}\left(\rho_{ve,a,e} - \rho_{ve,s,e} \right) \quad (2)$$

$$-\rho_l \left(D_T \frac{\partial T}{\partial x} + D_\theta \frac{\partial \theta}{\partial x} \right)\Bigg|_{x=L,i} = h_{M,i}\left(\rho_{ve,s,i} - \rho_{ve,a,i} \right) \quad (3)$$

The phase change occurring within porous materials acts as a heat source or sink, which results in the couple relationship between moisture and heat transfer. One dimensional of the energy conservation equation with coupled temperature and moisture for a porous media is considered, and the effect of the absorption or desorption heat is added. This equation is written as:

$$\rho_0 Cp_m \frac{\partial T}{\partial \tau} = \frac{\partial}{\partial x}\left(\lambda \frac{\partial T}{\partial x} \right) + L_v \rho_l \left(\frac{\partial}{\partial x}\left(D_{T,v} \frac{\partial T}{\partial x} \right) + \frac{\partial}{\partial x}\left(D_{\theta,v} \frac{\partial \theta}{\partial x} \right) \right) \quad (4)$$

$$Cp_m = Cp_0 + Cp_l \frac{\rho_l}{\rho_0}\theta \quad (5)$$

Where Cp_m is the average specific heat which takes into account the dry material specific heat and the contribution of the specific heat of liquid phase. λ is the thermal conductivity depending on moisture content.

Boundary conditions take into account radiation, heat and phase change.

$$-\lambda \frac{\partial T}{\partial x} - L_v \rho_l \left(D_{T,v} \frac{\partial T}{\partial x} + D_{\theta,v} \frac{\partial \theta}{\partial x} \right)_{x=0,e} = h_{T,e}\left(T_{a,e} - T_{s,e} \right) + L_v h_{M,e}\left(\rho_{ve,a,e} - \rho_{ve,s,e} \right) + \Phi_{ray,e} \quad (6)$$

$$-\lambda \frac{\partial T}{\partial x} - L_v \rho_l \left(D_{T,v} \frac{\partial T}{\partial x} + D_{\theta,v} \frac{\partial \theta}{\partial x} \right)\Bigg|_{x=L,i} = h_{T,i}\left(T_{s,i} - T_{a,i} \right) + L_v h_{M,i}\left(\rho_{ve,s,i} - \rho_{ve,a,i} \right) + \Phi_{ray,i} \quad (7)$$

In case of multilayered walls, we assume perfect contact on the contact interface. Neglecting moisture and thermal resistances at the interface between the porous materials, it is possible to state that temperature and capillary pressure are continuous (Mendes, 2003):

$$\begin{cases} (T)_A = (T)_B \\ (\psi)_A = (\psi)_B \end{cases} \quad (8)$$

Where T is the temperature and ψ is the capillary pressure.

According to Kelvin's law, we have:

$$\phi = \exp\left(\psi g / R_v T \right) \quad (9)$$

By using the equation (8), we can deduce:

$$\frac{R_v (T)_A}{g} \ln(\phi)_A = \frac{R_v (T)_B}{g} \ln(\phi)_B \quad (10)$$

Where R_v is the constant for water vapor, ϕ is the relative humidity and g is the gravity accelaration. Since the temperature for both materials are the same at the interface equation (10) turns into:

$$(\phi)_A = (\phi)_B \quad (11)$$

Which means that relative humidity is the same at the interface and moisture content for both materials are discontinuous because they have different pore structures.

Air model

The net heat transferred into the cell across its faces must equal the heat stored in the volume of air in the cell. That involves heat fluxes through the envelope (transmission, long and short-wave radiation input), additional thermal loads, air exchange due to natural convection or HVAC and thermal losses due to thermal heat bridges. The energy equation can be written as:

$$(\rho_i c_p V + I)\frac{\partial T}{\partial \tau} = \Phi_{West} - \Phi_{East} + \Phi_{South} - \Phi_{North} + \Phi_{Bottom} - \Phi_{Top} + \Phi_{Source} - \Phi_{Thermal\_bridge} \quad (12)$$

where I is room thermal inertia and $\Phi_{Thermal\_bridge}$ is the heat losses due to linear thermal bridges and it is given by:

$$\Phi_{Thermal\_bridge} = \sum L_j \psi_j \left(T_i - T_o\right) \qquad (13)$$

Where ψ_j is the thermal linear transmittance of thermal bridge j (W/m.K) and L_j is the length of thermal bridge j.

The humidity condition in the room is due to moisture transfer from interior surfaces, moisture production rate and the gains or losses due to air infiltration, natural and mechanical ventilation as well as sources or sinks due to habitants of room. This yields to the following mass balance equation for room air:

$$V\frac{\partial \rho_i}{\partial \tau} = Q_{mWest} - Q_{mEast} + Q_{mSouth} - Q_{mNorth} + Q_{mBottom} - Q_{mTop} + Q_{mSource} \qquad (14)$$

Radiation exchange in the room

In this article, we used the mean radiant temperature method to calculate long wave radiation exchange between walls. A linear equation expressing the radiative flow between a wall and all the other walls of the room is written as:

$$\Phi_{rad,LW}^{int} = h_r S\left(T - T_m\right) \qquad (15)$$

The value of h_r is expressed by:

$$h_r = 4\varepsilon\sigma_0 T_m^3 \qquad (16)$$

Where T_m is the mean radiant temperature of the walls and is given by:

$$T_m = \frac{\Sigma S_j T_{Sj}}{\Sigma S_j} \qquad (17)$$

For the shorts-wave radiation, we assumed that radiant energy enters the room by pane window and is distributed by the quota of 0,6 for the floor and 0,1 for the other walls.

Thermal comfort

Human thermal comfort is defined as that condition of mind that expresses satisfaction with the thermal environment. Simulation of energy consumption of buildings on hourly basis is closely connected to the thermal indoor climate. The operative temperature is used as a simple measure for thermal environment. The operative temperature is a function of the air temperature, the mean radiant temperature and the relative air velocity and can be expressed as:

$$T_0 = aT_a + (1-a)T_m \qquad (18)$$

Where: a is a coefficient depending on air speed (m/s) and it is given in table 1.

Table 1

Coefficient a

V (m/s)	0-0,2	0,2-0,6	0,6 – 1
Coefficient a	0,5	0,6	0,7

OBJECT – ORIENTED SIMULATION

Numerical resolution

In order to solve the previous equation system, the numerical solution is based on the finite difference technique with an implicit scheme thus unconditionally stable. We note ΔX and ΔT respectively the space and time steps. K_j^n represents the scalar value K of node j and at the time n.

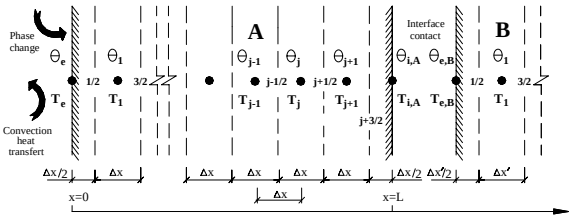

Figure 1 Discretization scheme

Figure 1 shows the discretization scheme of a double-layered wall as well as the interface between two walls A and B. Equation (1) can be written as:

$$\left(\frac{\Delta x^2}{\Delta t} + D_{\theta,j+1/2}^{n+1} + D_{\theta,j-1/2}^{n+1}\right)\theta_j^{n+1} - D_{\theta,j+1/2}^{n+1}\theta_{j+1}^{n+1} - D_{\theta,j-1/2}^{n+1}\theta_{j-1}^{n+1} + \left(D_{T,j+1/2}^{n+1} + D_{T,j-1/2}^{n+1}\right)T_j^{n+1} - D_{T,j+1/2}^{n+1}T_{j+1}^{n+1} - D_{T,j-1/2}^{n+1}T_{j-1}^{n+1} = \theta_j^n \qquad (19)$$

Equation (4) can be discretized implicitly as:

$$\frac{\Delta t}{\rho_0 Cp_m^{n+1}\Delta x^2}\left(\lambda_{j+1/2} + \lambda_{j-1/2} + L_v\rho_l D_{T,v,j+1/2} + L_v\rho_l D_{T,v,j-1/2} + \frac{\rho_0 Cp_m \Delta x^2}{\Delta t}\right)^{n+1} T_j^{n+1} - \frac{\Delta t}{\rho_0 Cp_m \Delta x^2}\left(\lambda_{j+1/2} + L_v\rho_l D_{T,v,j+1/2}\right)^{n+1} T_{j+1}^{n+1} - \frac{\Delta t}{\rho_0 Cp_m^{n+1}\Delta x^2}\left(\lambda_{j-1/2} + L_v\rho_l D_{T,v,j-1/2}\right)^{n+1} T_{j-1}^{n+1} - \frac{\Delta t}{\rho_0 Cp_m^{n+1}\Delta x^2}\left[D_{\theta,v,j+1/2}^{n+1}\theta_{j+1}^{n+1} - \left(D_{\theta,v,j+1/2} + D_{\theta,v,j-1/2}\right)^{n+1}\theta_j^{n+1} + D_{\theta,v,j-1/2}^{n+1}\theta_{j-1}^{n+1}\right] = T_j^n \qquad (20)$$

Concerning the boundary condition, equation (2) can be discretized as:

$$-\rho_l\left(D_{T,1/2}^{n+1}\frac{T_1^{n+1}-T_e^{n+1}}{\Delta x}+D_{\theta,1/2}^{n+1}\frac{\theta_1^{n+1}-\theta_e^{n+1}}{\Delta x}\right)$$
$$=h_{M,e}\left(\rho_{ve,a,e}^{n+1}-\rho_{ve,s,e}^{n+1}\right) \quad (21)$$

Concerning the energy equation of air room, we have

$$(\rho_i c_p V+I)\frac{T_{cell}^{n+1}-T_{cell}^{n}}{\Delta t}=\Phi_{West}^{n+1}-\Phi_{East}^{n+1}+\Phi_{South}^{n+1}$$
$$-\Phi_{North}^{n+1}+\Phi_{Bottom}^{n+1}-\Phi_{Top}^{n+1}+\Phi_{Source}^{n+1}-\Phi_{Thermal\_bridge}^{n+1} \quad (22)$$

And equation 13 can be written as:

$$V\frac{\rho_{cell}^{n+1}-\rho_{cell}^{n}}{\Delta t}=Q_{mWest}^{n+1}-Q_{mEast}^{n+1}+Q_{mSouth}^{n+1}-$$
$$Q_{mNorth}^{n+1}+Q_{mBottom}^{n+1}-Q_{mTop}^{n+1}+Q_{mSource}^{n+1} \quad (23)$$

Simulation Environment SPARK

To solve this system of equations we used the Simulation Problem Analysis and Research Kernel (SPARK), a simulation environment allowing to solve efficiently differential equation systems ((Sowell et al., 2001), (Mora et al., 2002), (Mendonça et al., 2002)). SPARK was developed by the Simulation Research Group at Lawrence Berkeley National Laboratory. Description of a problem for SPARK solution begins by breaking it down in an object-oriented way. This means thinking about the problem in terms of its component is represented by a SPARK object. A model is than developed for its component. Since there may be several components of the same kind, SPARK object models, equations or group of equations, are defined in a generic manner called classes. Classes serve as templates any number of objects required to formulate the whole problem. The problem model is then completed by linking objects together. Using graph theoretic techniques, SPARK reduce the size of the equation system and use a Newton-Raphson iterative method to solve the reduced system and after convergence, solves for the remaining unknowns. We have just presented the physical model which was implemented in SPARK, next we present simulations.

Simulations

First study

In the first study, in which we take only heat transfer in building (**Th** model), we compared three cases: a hemp concrete envelope room, a normal concrete room with external insulation and a normal concrete room with internal insulation. The plan of studied rooms is depicted in figures 2 and 3. The room has a space area of 15 m^2 and a volume of 42,75 m^3. Southern façade is made of double glazing. The ceiling, the west and south facades are in contact with outdoor conditions while other walls are considered as internal partitions and in contact with heated space at 20 °C temperature and 60 % relative humidity. External walls and ceiling have 30 cm thickness and partitions 20 cm. For the hemp concrete room, western wall and the ceiling are made of a triple layer of 28 cm of hemp concrete and two layers of 10 mm of mortar from the inside and outside faces (figure 2).

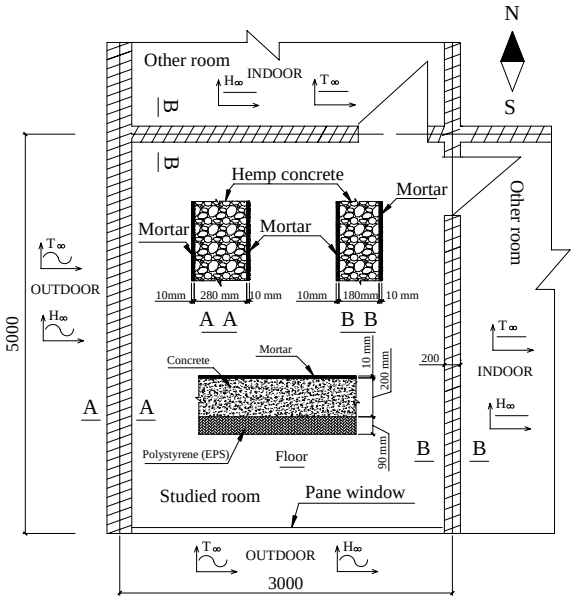

Figure 2 Plan of the hemp concrete studied room.

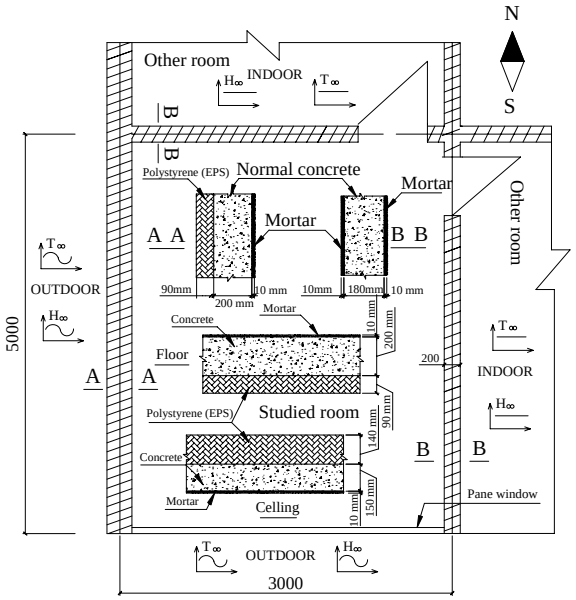

Figure 3 Plan of the studied room made by normal concrete

The same thickness was kept for normal concrete room with 20 cm of concrete, 9 cm of polystyrene insulator and 10 mm of mortar. For the ceiling, we used 14 cm of polystyrene, 15cm of concrete and 10 mm of mortar (figure 3).

The room is equipped with a heat sink and a PI controller that keeps operative temperature around 20 °C. Room is ventilated at 0,5 Ach. Heat transfer coefficients are $h_{T,e}$= 25 W/m^2.K for the outdoor surfaces and $h_{T,i}$= 6 W/m^2.K for indoor surfaces. The initial relative humidity and temperature in the walls and the studied room were respectively equal to 60 % and 20 °C. Simulations are run for three monthes in winter condition with Nancy weather data (in France). The mortar layers and insulations are discretized in 5 nodes and the other layers are divided into 10 nodes. Time step is 240 s.

Computed results

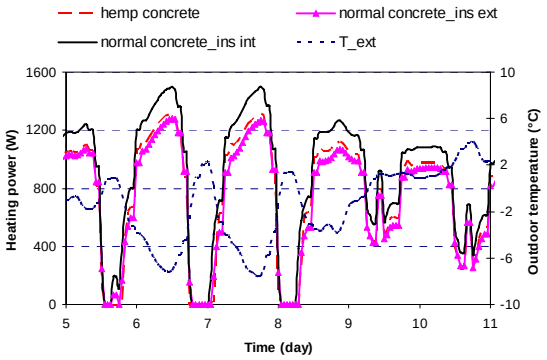

Figure 4 Variation of the input heating power for the three cases: hemp concrete, normal concrete with internal and external insulation.

Figure 4 shows the variation of the input heating power for the three studied cases. We can notice that for the hemp concrete envelope, the input energy is slightly higher than the case of normal concrete with external insulation. This is due to the ceiling conductance, which is lower for the normal concrete case. Concerning the case of internal insulation, the input energy is higher due to the thermal bridges. This shows that hemp concrete has a satisfying thermal behaviour and it can be used to reduce heating energy consumption. Though hemp concrete is normally used in combination with a timber frame, this framing does not behave as a thermal bridge because hemp concrete and wood have similar thermal properties.

Regarding the total energy consumption, it is shown in Figure 5. Here again, hemp concrete building energy demand is close to external insulation normal concrete building. It is 4,4 % higher than the external insulation case and 19 % lower than internal insulation case. Actually, in France, internal insulation is more commonly used than external insulation because it is less expansive and easier to be installed. In the next section, we will present the **HAM**'s model results.

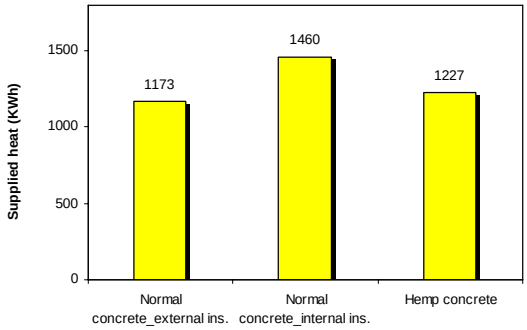

Figure 5 Heat supplied (KWh) for three months in winter for different models

Second study

In this study, we considered heat and mass transfer in hemp concrete envelope; the same building shown in figure 2 was used. Equations of the HAM model presented in the second section were used.

Table 1

Properties of hemp concrete and normal concrete at T=20°C and 60% relative humidity

Hemp concrete						
Density	Thermal Conductivity	Specific heat	D_Θ	D_T	$D_{\Theta v}$	D_{Tv}
kg/m^3	*W/m.K*	*J/kg.K*	*m^2/s*	*m^2/(s.K)*	*m^2/s*	*m^2/(s.K)*
413	0,11	1000	3,5E-9	2E-13	3,4E-9	2E-13
Normal concrete						
Density	Thermal Conductivity	Specific heat	D_Θ	D_T	$D_{\Theta v}$	D_{Tv}
kg/m^3	*W/m.K*	*J/kg.K*	*m^2/s*	*m^2/(s.K)*	*m^2/s*	*m^2/(s.K)*
2300	1,6	850	1,3E-9	1,6E-14	4,5E-11	1,6E-14

Mortar input data (material properties, sorption isotherms, moisture diffusion coefficients) were obtained from Perrin (Perrin, 1985). The input data of hemp concrete and normal concrete were taken from ((Collet, 2004), (Cerezo, 2005), (WUFI)) as shown in Table 2 and Figure 6. Room is occupied by one person from 9 AM till noon and from 1 PM to 6 PM. No other moisture sources were considered.

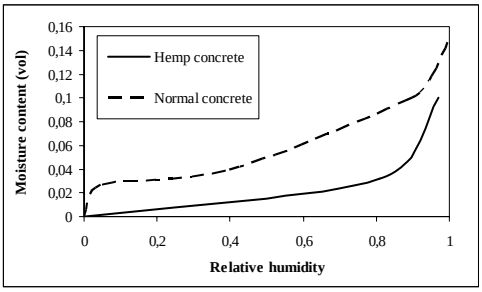

Figure 6 Sorption isotherms of hemp concrete and normal concrete

Mass transfer coefficients were calculated using the Lewis number relation:

$$Le = \frac{h_t}{h_m \rho C_p} = 1 \qquad (24)$$

Computed results

Figure 7 shows the variation of indoor input heating energy for both models **Th** and **HAM**. We notice that energy variation is small. When indoor moisture density is higher than wall surface moisture density, energy input for the **HAM** model is slightly lower than Th model's input because of the adsorption process due to vapour movement from indoor air to wall surfaces. This occurs during the day when the room is occupied. During the night, the desorption phenomenon occurs, and heating power is slightly higher. The total energy consumption is too close for both models. For the HAM model, it is equal to 1243 kWh compared to 1227 kWh for the Th model.

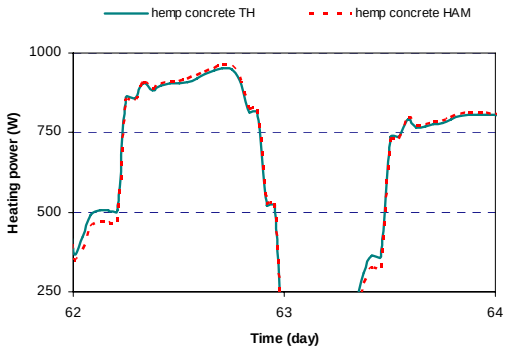

Figure 7 Variation of input heating power for both HAM and Th model

Figure 8 presents indoor relative humidity pattern for both models. We observe that taking into account moisture transfer through the envelope dampens indoor relative humidity variation. In this case, a difference of 25 % can be reached between the two models.

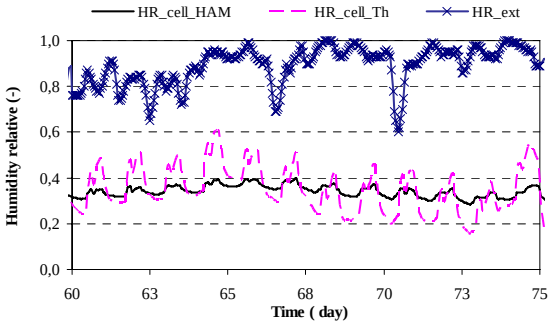

Figure 8 Variation of indoor air relative humidity during fifteen days of March.

Table 3 summarizes the results of computed indoor relative humidity for the two models. In winter, the indoor humidity for the **HAM** model varies between (28 % - 57 %) compared to (15 % - 61 %) of the **Th** model. It is clear that neglecting water vapour transport between air and the material can lead to big errors in estimating the indoor air humidity. The values of indoor relative humidity are lower than 40 % which could lead to some levels of occupant discomfort but this is normal because we considered no moisture production sources in the room (only one person for 8 hours per day).

Table 2

*Maximum, minimum and average indoor relative humidity of studied room made of hemp concrete for the models **HAM** and **Th** and outdoor relative humidity in winter*

Model	**HAM**	**Th**	**Outdoor HR**	
HR_cell_max	0,57	0,61	HR_ex_max	1,00
HR_cell_min	0,27	0,15	HR_ex_min	0,54
HR_cell_average	0,32	0,35	HR_ex_average	0,87

CONCLUSION AND PERSPECTIVES

In this paper, the interaction between a multilayered hemp concrete envelope and indoor air is investigated. The results for the **Th** model are then compared with the normal concrete. We presented a one-dimension model for heat and moisture transfer through a triple layer wall. The numerical solution is based on the finite difference technique and the system of equations was implemented in SPARK, an object-oriented program suited to complex problems. The computed results show that neglecting moisture transport between air and material can lead to serious errors in estimating the indoor air relative humidity. In case of a constant air flow no differences on heating demand were found. It seems important to study the case of a relative humidity sensitive ventilation system. Compared to normal concrete,

hemp concrete envelope has a low energy consumption in winter like an outdoor insulation envelope. However, low hemp concrete density may affect its thermal storage behaviour and this aspect should be investigated. Besides summer thermal comfort should be studied especially under long heat-wave periods.

NOMENCLATURE

Symbol	Definition	Unity
C	Specific heat	$J.kg^{-1}.K^{-1}$
C_0	Specific heat of dry material	$J.kg^{-1}.K^{-1}$
C_l	Specific heat of water	$J.kg^{-1}.K^{-1}$
D_T	Mass transport coefficient associated to a temperature gradient	$m^2.s^{-1}.K^{-1}$
$D_{T,v}$	Vapor transport coefficient associated to a temperature gradient	$m^2.s^{-1}.K^{-1}$
D_θ	Mass transport coefficient associated to a moisture content gradient	$m^2.s^{-1}$
$D_{\theta v}$	Vapor transport coefficient associated to a moisture content gradient	$m^2.s^{-1}$
g	Gravity acceleration	$m^2.s^{-1}$
h_M	Mass transfer convection coefficient	$kg.m^{-2}.s^{-1}$
h_T	Heat transfer convection coefficient	$W.K^{-1}.m^{-2}$
L_v	Heat of vaporization	$J.kg^{-1}$
R_v	Constant of water vapor	$J.kg^{-1}.K^{-1}$
T	Temperature	K
Ta	Indoor air temperature	K
T_m	mean radiant temperature of the walls	K
To	operative temperature	K
t	Time	s
x	Abscise	m
θ	Moisture content	$m^3.m^{-3}$
λ	Thermal conductivity	$W.m^{-1}.K^{-1}$
ρ_0	Mass density of dry material	$kg.m^{-3}$
ρ_l	Mass density of water	$kg.m^{-3}$
ρ_v	Mass density of vapor water	$kg.m^{-3}$
ψ	Capillary pressure	Pa
ψ_{tb}	Linear thermal bridge coefficient	$W.m^{-1}.K^{-1}$
ϕ	Relative humidity	%
ρ_i	Air density	$kg.m^{-3}$
Φ	Heat flux	W
Q_m	Air flow rate	$Kg.s^{-1}$
Φ_{source}	Heat source power	W
ε	Wall emissivity (long wave)	
σ_0	Stephan-Boltzmann constant	$W.m^{-2}.T^{-4}$

REFERENCES

Cerezo V. 2005. Propriétés mécaniques, thermiques et acoustiques d'un matériau à base de particules végétales : approche expérimentale et modélisation théorique, Thèse de Doctorat, INSA & ENTPE de Lyon, 242 p.

Collet F. 2004. Caractérisation hydrique et thermique de matériaux de génie civil à faibles impacts environnementaux, Thèse de Doctorat, INSA de Rennes, 220 p.

Elfordy, S., Lucas F., Tancret, F., Scudeller, Y., Goudet, L. 2007. Mechanical thermal properties of lime and hemp concrete (« hemp Crete ») manufactured by a projection process, Construction and Building Materials, (Article in press).

Hameury S. 2005. Moisture buffering capacity of heavy timber structures directly exposed to an indoor climate: a numerical study. Building and Environment (40) (2005), p.1400-1412.

Kunzel M. 1995. Simultaneous heat and moisture transport in building components, Fraunhofer Institute of building physics, Allemagne, 1995, disponible sur:
http:// www.wufi.de/index_e.html (section: Literatur).

Kwiatkowski, J., Woloszyn, M., Roux, J.J. 2009. Modelling of hysteresis influence on mass transfer in building materials. Building and Environment (44) (2009), p.633-642.

Mendes N. 1997. Models for prediction of heat and moisture transfer through porous building element, Thèse de doctorat, 225, Federal University of Santa Catarina, Florianopolis, SC, Brésil.

Mendes, N., Winkelmann, F.C., Lamberts, R., Philippi. 2003. Moisture effects on conduction loads, Energy and Buiding, v. 35, n. 7, p.631-644.

Mendonça, K.C., Inard, C., Wurtz, E., Winkelmann, F.C., Allard, F. 2002. A zonal model for predicting simultaneous heat and moisture transfer in buildings, Indoor Air 2002, 9th International Conference on Indoor Air Quality and Climate, Monterey, USA, 2002.

Mora, L., Wurtz, E., Mendonça, K.C., Inard, C. 2002 .Simspark: an object oriented environment to predict coupled heat and mass transfers in buildings, Building Simulation'03 Conference, Eindhoven, Pays-Bas, 2003, p.903 - 910.

Olalekan, F. O., Simonson, C. J. 2006. Moisture buffering capacity of hygroscopic building materials: Experimental facilities and energy impact. Energy and Building (38) (2006), p.1270-1282.

Pedersen C.R. 1992. Prediction of moisture transfer in building constructions, Building and Environment (3) (1992), p.387–397.

Perrin B. 1985. Etude des transferts couplés de chaleur et de mass dans des matériaux poreux consolidés non saturés utilisés en génie civil. Thèse Docteur d'Etat, Université de Paul Sabatier de Toulouse, Toulous, France.

Philip, J.R., De Vries, D.A. 1957. Moisture movement in porous materials under temperature gradients, Transaction of American Geophysical Union. V.38, n.2, p.222-232.

Sowell, E.F., Haves, P. 2001. Efficient solution strategies for building energy system simulation, Energy and Buildings, vol. 33, p. 309-317.

WUFI. Wärme und Feuchte instationär consultable sur:http://www.wufi.de/index_e.html (section: Basics, Moisture Storage Function).